

## Investigation of electrocoagulation on the removal of nickel in waste water from an electroplating bath using aluminium and iron electrodes

Sarah Jerroumi<sup>(1,2)</sup>, Stenelvie NGALA<sup>(2,3)</sup>, Brahim Lekhlif<sup>2</sup>, Jamal Eddine Jamal<sup>1</sup>, Mahjoub Lakhdar<sup>1</sup>, Lahcen Afrine<sup>4</sup>

(1) Extraction, valorisation and spectroscopic studies. Laboratory of organic synthesis, extraction and valorization. Faculty of sciences Ain Chock, Hassan II University, Route d'El Jadida Km 2, BP: 5366, Casablanca Morocco.

(2) Research team Hydrogeology, Water Treatment and Climate Change. Environment Engineering Laboratory. Hassania School of public works. Route d'El Jadida, km 7, BP: 8108, Casablanca, Morocco.

(3) Higher National School of Mechanics and Electricity, Hassan II University. Route d'El Jadida, km 7, BP: 8118, Casablanca, Morocco.

(4) Maroc Bureau. Km 9.8 Route de rabat 20250, Casablanca, Morocco.

### Abstract

The electrocoagulation (EC) has proven its effectiveness in the treatment of industrial effluents by the elimination of pollutants, especially metallic pollutants. The electrochemical processes that occur at the electrodes (aluminum or iron) give an excellent performance. In this work, EC tests were conducted on an industrial effluent from an electroplating bath. The goal is to eliminate the Nickel and reuse the purified water for other needs within the company. For this purpose, we proceeded to the optimization of the operating parameters acting on the efficiency of EC such as electric voltage, material of the electrode, stirring speed and interelectrode distance. We also evaluated these parameters' effect on pH, conductivity, turbidity and nickel concentration. The tests were carried out in a perfectly stirred reactor on an industrial solution rich on nickel. The concentration of the effluent is 100 mg Ni<sup>2+</sup>/L. The nickel removal efficiency is approximately 78% for the following operating conditions: aluminum electrodes, regulated voltage of 6 volts, optimum stirring speed of 24 rpm and interelectrode distance of 2 cm. Resulting sludges from EC were characterized by X-ray diffractometry, infrared spectroscopy (IR) and scanning electron microscopy (SEM). We have identified a compound formed during the EC with Fe/Fe electrodes (Fe<sub>2</sub>Ni<sub>2</sub>(CO<sub>3</sub>) (OH)<sub>8</sub> .2H<sub>2</sub>O (Nickel Iron Carbonate Hydroxide Hydrate) which is a corrosion inhibitor.

\* Corresponding author:

[sarah\\_jerroumi@hotmail.com](mailto:sarah_jerroumi@hotmail.com)

Received 27 May 2019,

Revised 30 Aug 2019,

Accepted 04 Dec 2019

**Keywords:** nickel; electrocoagulation; aluminum; iron

## 1. Introduction

The presence of high concentrations of heavy metals in the discharges of electroplating industries can have detrimental impact on the environment and human health. To ensure their elimination, different treatment techniques can be used, taking into account their advantages and limitations [1]–[6]. Electrocoagulation (EC) is one of the most widely used techniques in the industrial sector, because it eliminates a wide range of pollutants present in different types of wastewater, such as aqueous suspensions [7]; fluoride [8], heavy metals [9]; black liquor [10], oils [11]; phenolic waste [12], water from textile industries [13], etc. According to Haase [14], electrochemical techniques are advantageous because they are adapted to the environment and are characterized by an affinity to different pollutants, good energy efficiency, safety, selectivity, adaptability to automation and profitability. In addition, systems operating with EC process are fast and viable involving only electrons for wastewater treatment [15].

### *Theory of electrocoagulation :*

EC is an electrochemical technique that consists of an electrolysis cell composed of two electrodes, an anode and a cathode. This cell is subjected to a continuous voltage, generating a current allowing the dissolution of soluble anodes and thus forming cations allowing coagulation *in situ* (Reaction 1). The electric field allows simultaneous formation of hydroxyl ions and hydrogen gas at the cathode (Reaction 2). The most commonly used metals are iron and aluminum [16] because of their slower costs and higher valence. The main reactions taking place within the electrolyser are:

#### At the anode :

Oxydation of metal :  $M \rightarrow M^{n+} + ne^-$  (Reaction 1)

#### At the cathode :

Reduction of water :  $2 H_2O (l) \rightarrow H_2 (g) + OH^-$  (Reaction 2)

The generated metal cations can be hydrolyzed (Reaction 3), and subsequently give rise to several monomeric hydrolyzed complexes, positively charged ( $M(OH)_x^{(y-x)+}$ ), which can eventually be transformed into polymer complexes such as hydroxide ( $M_x(OH)_y^{(x*n-y)+}$ ) or oxohydroxyde ( $M_x(O)_y(OH)_z^{(x*n-2y-z)+}$ ).

$M^{n+} + xH_2O \rightarrow M(OH)_x^{(n-x)+} + xH^+$  (Reaction 3)

The presence of these structures depends on the pH of the environment [15], [17]. They can electrostatically aggregate and destabilize a number of negatively charged pollutants, such as colloidal material, by compressing the diffuse double layer surrounding these particles, reducing the repulsive forces (negative Zeta potential) [9], [18].

$2H_2O \rightarrow O_2 + 4H^+ + 4e^-$  (Reaction 4)

During EC, the pH of the medium increases. This can lead to the precipitation of  $M(OH)_n$  which is formed from the metal polymers present in the solution (Reaction 5).

$M_x(OH)_y^{(x*n-y)+} + (x*n-y) OH^- \rightarrow xM(OH)_n$  (Reaction 5)

In basic medium, other solids may be formed in addition to  $M(OH)_n$  precipitates [19]. All these solid compounds allow the coagulation of the colloidal material by adsorption. When the pH increases further,  $M(OH)_n$  can react with the  $OH^-$  ions to produce negatively charged hydroxyl complexes, which reduces the coagulation of the colloidal particles.

The aim of this work is the treatment of an effluent from an electroplating industry by EC, to evaluate their performance, through a certain number of monitoring parameters such as electrical voltage, electrode nature, interelectrode distance and stirring speed. Sludge resulting from the EC will be analyzed by X ray diffraction (XRD) and Infrared Spectroscopy (IR) to characterize their crystallographic structure and scanning electron microscopy (SEM) to identify the morphology of the formed compounds. The electrodes used are aluminum (Al/Al) and iron (Fe/Fe).

## 2. Materials and methods

The EC tests are conducted in an effluent taken from a rinsing bath of metallic parts of an electroplating unit. Rectangular electrodes with identical dimensions (1.5 cm in width, 20 cm in length and 1 mm in thickness) are immersed in parallel in an electrolytic cell containing a volume of 200 ml of the solution. The EC reactor is fed by a direct current (DC) generator. The agitation of the solution was provided by a magnetic stirrer in order to prevent the deposit of the flocs on the bottom and the walls of the reactor. Before each experiment, the aluminum and iron electrodes are previously polished with fine abrasive paper and then washed in an aqueous solution of hydrochloric acid HCl (2M) to remove the passivation layer formed on the surface (formation of metal oxides:  $\text{Al}_2\text{O}_3$  and  $\text{Fe}_3\text{O}_4$ ).

To optimize the efficiency of the EC, we proceeded to the variation of only one factor at a time (Material of electrode, electric tension, speed of agitation and distance between electrodes), while maintaining the others constant. It should be noted that the initial concentration of nickel  $[\text{Ni}^{2+}] = 100 \text{ mg/L}$  remains invariable during all tests. For a best monitoring of the parameters' performance, 20 ml of samples were taken every five minutes during 20 minutes. The samples taken are filtered with membrane filters (0.45  $\mu\text{m}$ ) and preserved with a few drops of nitric acid (70%) (Aldrich) before being analyzed. For each sample, the nickel concentration was measured three times to determine the average concentration in terms of reproducibility and repeatability. All tests were performed at room temperature (28 °C) and are summarized in Table 3.

**Table 1** Parameters in each electrocoagulation test

	<b>Test 1</b>		<b>Test 2</b>	<b>Test 3</b>
<b><math>[\text{Ni}^{2+}]</math> (mg/l)</b>	100	100	100	100
<b>Temperature (°C)</b>	28	28	28	28
<b>Voltage (V)</b>	<b>3-8</b>	<b>3-8</b>	6	6
<b>Stirring speed (tr/min)</b>	24	24	<b>0-75</b>	24
<b>Inter-electrodes distance (cm)</b>	2	2	2	<b>1-3</b>
<b>Material</b>	Aluminium	Iron	Aluminium	Aluminium

## 3. Results and discussion

### 3.1 Test 1: Effect of the applied voltage and the nature of the electrodes.

In this test, we applied a DC voltages varying between 3 and 8 volts. During the test, the pH, the conductivity and the residual nickel concentration are measured for each type of electrode.

#### 3.1.1 Concentration of nickel

Figure 1 shows that when the applied voltage to the electrodes increases, the nickel concentration decreases, confirming the results of several authors [20]–[22]. However, the reduction of nickel is better in the case of Al/Al electrode pair. Indeed, for a voltage of 8V, the nickel removal efficiency reached 85% for Al/Al electrodes pair and 76% for Fe/Fe electrodes pair after 20 minutes of EC with residual concentrations of  $\text{Ni}^{2+}$  15 mg and 23 mg/l respectively. Beyazit [21] showed concordant results in a comparative tests between the Al/Al and Fe/ Fe electrodes. The increase of the voltage between the electrodes makes possible the increase of the electric current, by releasing more metal cations ( $\text{Al}^{3+}$ ,  $\text{Fe}^{3+}$ ) and  $\text{OH}^-$  in the solution. Therefore, it promotes better  $\text{Ni}^{2+}$  removal by precipitation in

the form of  $\text{Ni(OH)}_2$  (Heidmann and Calmano 2010), or probably by adsorption on the flocs of  $\text{Al(OH)}_3$  or other solids that may be formed during EC [22], or by co-precipitation with the oxides of Al and Fe [24].

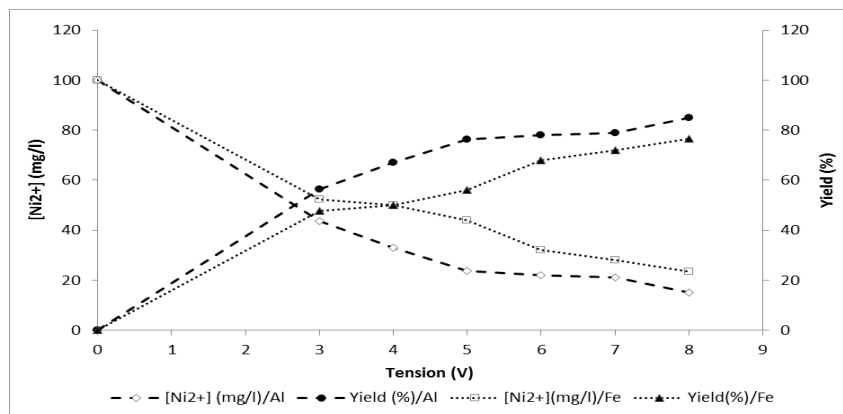


**Figure 1.** Nickel concentration and removal efficiency after 20 minutes of EC as a function of voltage for Al/Al electrodes and Fe/Fe electrodes

### 3.1.2 pH :

Figure 2 shows a decrease in pH during the EC for different applied voltages. This decrease is all the more marked as the tension is high. It is probably justified by the predominance of reactions releasing  $\text{H}^+$  protons (Reactions 3 and 4) at the expense of reactions releasing  $\text{OH}^-$  ions (Reaction 2), all of which may occur concomitantly. Many authors have shown that during EC, the pH increases when it is less than 7 and decreases when it is greater than 7 because of the amphoteric character of  $\text{Al(OH)}_3$  [25], [26].

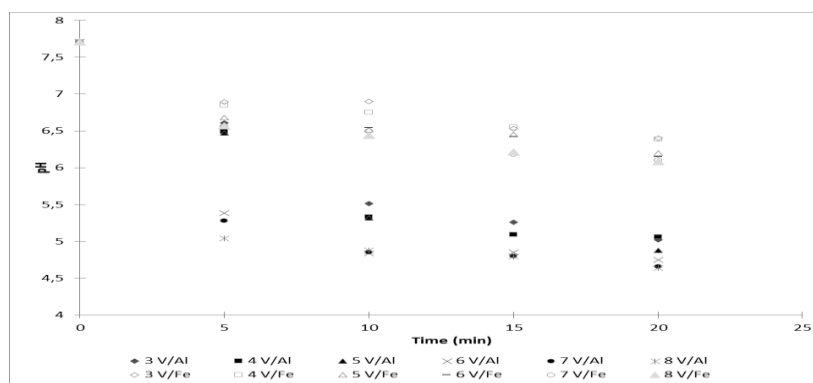


**Figure 2.** pH variation during EC as a function of time (Al/Al and Fe/Fe Electrodes)

Dermentzis et al. [27] has also conducted a study on the effectiveness of EC with aluminum electrodes to remove nickel from synthetic aqueous solutions and real wastewater. For a solution with a nickel concentration of 250 mg/L and an initial pH of 7.5, the authors found that the pH decreases and rises abruptly at the end of the treatment to reach a value approaching 8. The decrease in pH is more accentuated in the case of the Al/Al electrodes pair than in the case of the Fe/Fe electrodes pair. This is explained by an increased dissolution of the aluminum cathode. The factors that may explain this difference can be summarized as follow:

- The low standard potential of the  $\text{Al}^{3+}/\text{Al}$  redox couple (-1.66 V) compared to  $\text{Fe}^{3+}/\text{Fe}$  (-0.037 V) or  $\text{Fe}^{2+}/\text{Fe}$  (-0.447 V), which could promote rapid dissolution of the aluminum cathode;

- The dissolution of the iron cathode as  $\text{Fe}^{2+}$  [28], [29]; this low charge cation has a lower coagulant effect than  $\text{Al}^{3+}$ ;
- The high electrical mobility of  $\text{Al}^{3+}$ , favoring better conductivity than iron cations [30].
- This could be supported by the values of the conductivity of the  $\text{Al}^{3+}/\text{Al}$  pair of figure 3.

### 3.1.3 Conductivity :

The tests showed that the conductivity decreases during EC for different voltages (figure 3). This decrease is more pronounced in the case of Fe/Fe electrodes.

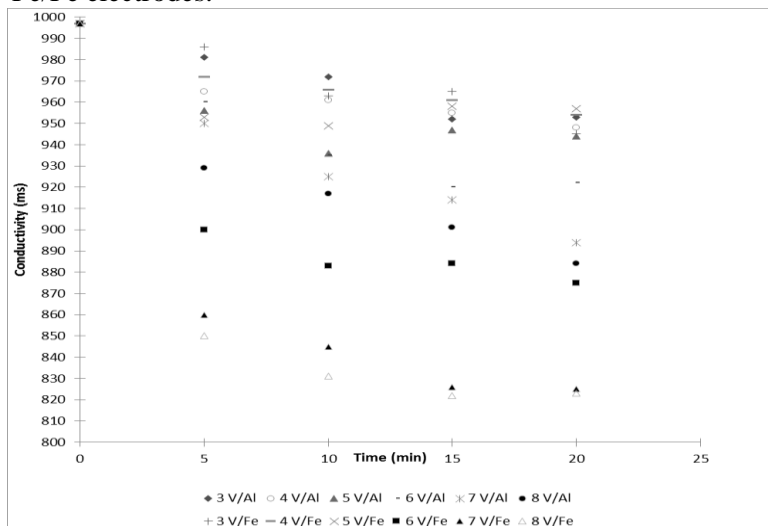


**Figure 3.** Variation of conductivity over time as a function of voltage (Al/Al and Fe/Fe Electrodes)

The decrease in conductivity is due to the removal of ions, including  $\text{Ni}^{2+}$ , by precipitation as confirmed. It can also be due to the adsorption of these ions on the flocs of precipitates and hydroxides of aluminum and iron formed during the EC [26]. In addition, many authors have shown that in the case of certain discharges treated by EC, the electrical conductivity decreases over time [21], [31]–[33]. They attributed this decrease to:

- Coagulation by metal ions ( $\text{Al}^{3+}$ ,  $\text{Fe}^{2+}$ ,  $\text{Fe}^{3+}$ ) in the form of metal hydroxides. The concentration of ions in the electrolyte becomes low because of the reduction of the negative ions.
- Formation of the polymers according to the reaction 3.
- The adsorption of  $\text{Ni}^{2+}$  on aluminum and iron hydroxides formed during EC.

The Al/Al pair gives a higher conductivity than Fe/Fe pair for the different applied voltages. This result is in fact confirmed by some authors [33]. This corroborates the best performance obtained with aluminum electrodes, including nickel abatement. Indeed, as the conductivity increases, the ion transfer improves further. This allows the removal of pollutants from releases, which is the goal of the treatment with EC. It is important to underline that the improvement of the  $\text{Ni}^{2+}$  ion abatement rate is not necessarily bigger by the application of electrical voltages greater than 6 volts. Therefore, the 6 volts voltage is considered as the optimal voltage for the rest of the tests.

### 3.2 Test 2: Effect of stirring speed

In EC tests with aluminum electrodes, the stirring speed was optimized with an optimum voltage of 6 volts. For this purpose, four speed values were used: 0, 24, 50, 75 rpm. After 20 min of EC, the residual nickel concentration was measured. The results of the tests are shown in Figure 4.

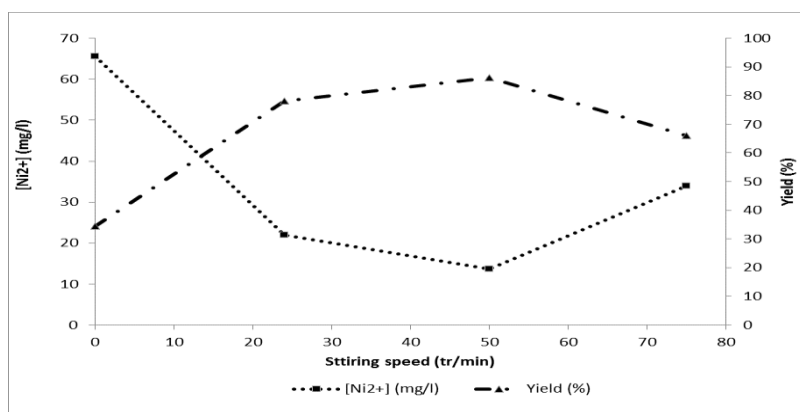


**Figure 4.** Concentration and yield of nickel removal as a function of stirring speed, after 20 minutes of EC

This figure shows that in the absence of mechanical agitation, the removal of nickel is low, its residual concentration is 65.57 mg/l, corresponding to a removal efficiency of 35%. When the stirring speed increases, this yield increases up to 87% for a stirring speed of 50 rpm, the residual concentration of nickel is equal to 13.73 mg/l. Above 50 rpm, the removal efficiency decreases. This may be due to the breakage of the flocs formed by rapid stirring, leading to the desorption of  $\text{Ni}^{2+}$  ions [28], [34]. The flocs thus formed are floated by the gases issuing from the two electrodes, which does not allow the reabsorption of  $\text{Ni}^{2+}$  despite the increase of the exchange surface. In order to study the settlability of the sludge formed during three EC tests carried out at three stirring speeds (0 - 24 - 50 rpm), we monitored the turbidity of the treated water as a function of time (figure 5). The results obtained show that for the three speeds, the turbidity decreases continuously over time but depends on the stirring speed. Decantation is faster for 24 rpm. In the case of the test carried out at 50 rpm, this settling is relatively lower. This could be explained by the formation of small flocs by mechanical shearing and/or electroflotation. This observation reinforces the conclusions made above and shows two antagonistic phenomena: firstly, an improvement in the elimination of  $\text{Ni}^{2+}$  by adsorption on the solid particles formed by EC and, secondly, a reduction in the elimination efficiency due to the increase of the stirring speed which would favor the electroflotation of the particles.

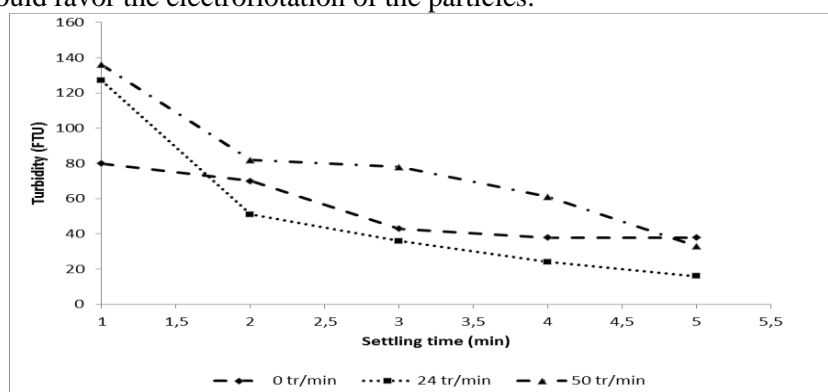


**Figure 5.** Variation of turbidity as a function of settling time for 3 stirring speeds (0 rpm, 24 rpm, 50)

### 3.3 Test 3: Effect of the interelectrode distance

The interelectrode distance has a considerable effect on the amount of electrical energy introduced into the EC cell to create an electric field [35]. This test aims to evaluate this effect by optimizing the distance between the two aluminum electrodes. This distance has been varied from 1 cm to 3 cm, the optimal values of the other parameters are kept constant.

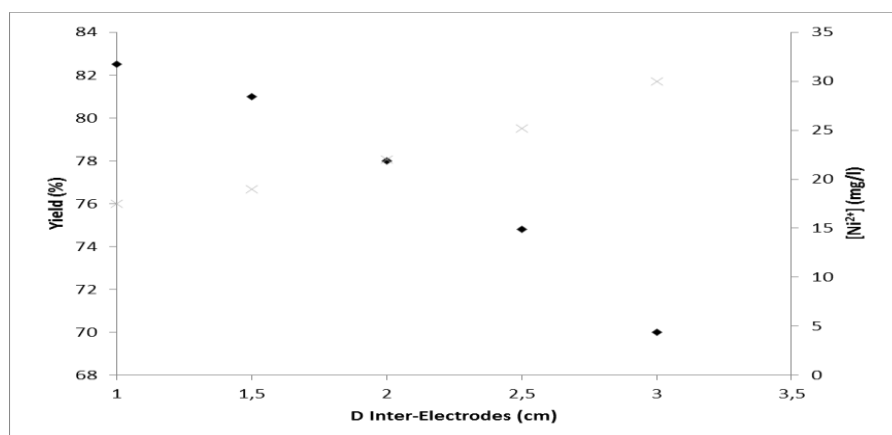


**Figure 6.** Nickel removal efficiency, after 20 min of EC, as a function of interelectrode distance at 6 volts

The nickel removal efficiency decreases as the interelectrode distance increases (figure 6). It goes from 82.5% for a distance of 1 cm to 70% for a distance of 3 cm. This can be explained by the increase in the ohmic drop when the distance between the electrodes increases [36], which causes a decrease in the ion transfer and consequently a decrease in the elimination efficiency. According to Meunier et al. [24] and to Missaoui et al. [32], increased distance leads to greater resistance to mass transfer and slower charge transfer kinetics, resulting in high energy costs. Moreover, when the interelectrode distance decreases, the nickel removal efficiency increases, which can be explained by the increase in electrostatic interactions according to the following equation :

$$IR = \frac{I * d}{S * K}$$

I: Intensity (Ampere)

d: distance between the electrodes (cm)

S: immersed surface of the electrode (cm<sup>2</sup>)

K: conductivity of the solution (S/cm).

### 3.4 Characterization of sludge :

Sludges resulting from EC treatments are recovered for characterization. These sludges are produced by precipitation of Ni(OH)<sub>2</sub> during the EC and those deposited on the aluminum cathode.

This sludge was oven dried and then subjected to three analytical techniques, namely X-ray diffraction (XRD), infrared spectroscopy (IR) and scanning electron microscopy (SEM).

#### 3.4.1 X-ray diffraction analysis:

The sludge resulting from EC with aluminum electrodes presents an X-ray diffractogram with broad bands (figure 7.a) corresponding to insufficiently crystallized phases that are difficult to identify by X-ray diffraction (XRD).

For the sample of the sludge deposited on the aluminum cathode, the X-ray diffractogram (figure 7. b) shows the presence of two phases, aluminum as a major phase and nickel. The latter is obtained by reduction of Ni<sup>2+</sup> ions at the cathode. In figures a and b, we expected the appearance of peaks characterizing the phase of nickel hydroxide, a green solid deposited on the cathode as shown by [15]. Moreover, this result can probably explain that the nickel hydroxide formed is an amorphous solid, resulting in the appearance of a few broad and diffuse peaks, typically corresponding to an amorphous phase that can not be identified by XRD. This hypothesis was supported by the results obtained by Duan et al.[37] and Prasetyaningrum [38] which confirm that the precipitate obtained by EC is amorphous.



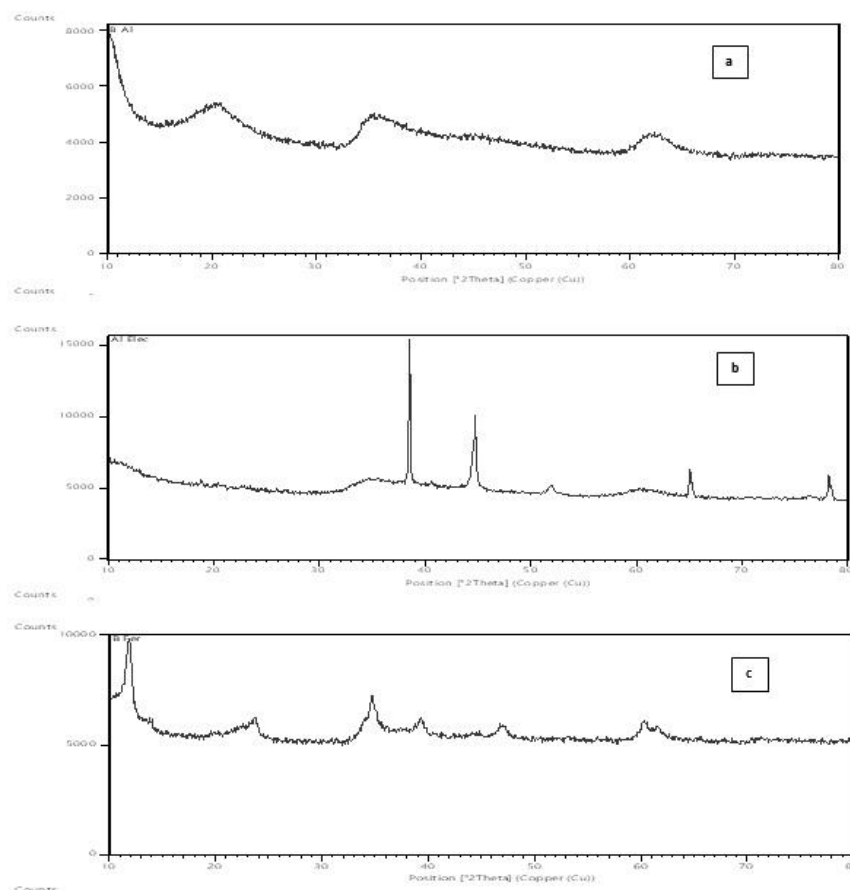


**Figure 7.** X-ray diffraction spectrum of the sludge produced by EC with a : Al/Al electrodes, b : Precipitate deposited on Al electrodes , c : Fe/Fe electrodes

The sludge resulting from EC with iron electrodes is characterized by a diffractogram (figure 7.c) identifying the following crystalline phase:  $\text{Fe}_2\text{Ni}_2(\text{CO}_3)(\text{OH})_8 \cdot 2\text{H}_2\text{O}$  (Nickel Iron Carbonate Hydroxide Hydrate) crystallizing in a hexagonal system. This compound, discovered by Uzunova et al. [39], is known as a corrosion inhibitor. Also, during EC, its formation can inhibit the oxidation of iron. This may explain the low nickel removal efficiency with iron electrodes.

### 3.4.2 Infrared Spectroscopy Analysis :

Figure 8 shows the IR spectra obtained for the three sludges studied. In this figure, we notice for the sludge formed by EC with Al/Al electrodes (figure 8.a) and the sludge deposited on the cathode Al (figure 8.b) respectively the presence of a:

- Wide band at  $3448\text{ cm}^{-1}$  and  $3446\text{ cm}^{-1}$  which probably correspond to an OH vibration of hydroxyl groups bound to hydrogen and intercalated by water molecules located in the interlamellar spaces of  $\text{Ni}(\text{OH})_2$  [40], [41] ;
- $1161\text{ cm}^{-1}$  and  $1641\text{ cm}^{-1}$  bands characteristic of an OH vibration[40], [42];
- Low band at  $615\text{ cm}^{-1}$  and  $657\text{ cm}^{-1}$  characteristic of a vibration of the Ni-OH bond [40], [41].

These vibrations are in agreement with the amorphous structure identified by X-ray diffraction. Indeed, according to Li et al. (2013) the compound characterized by IR corresponds to amorphous  $\text{Ni}(\text{OH})_2$ .

Sludges resulting from EC with Fe/Fe electrodes (figure 8.c) show:

- Band at  $3465\text{ cm}^{-1}$ , which can be attributed to an extensional vibration of a hydroxyl group O-H,



- Band at 1637 which can be attributed to a deformation vibration of the hydroxyl group of water,
- Band at 1377 cm<sup>-1</sup> probably corresponding to the vibration of CO<sub>3</sub><sup>2-</sup>.

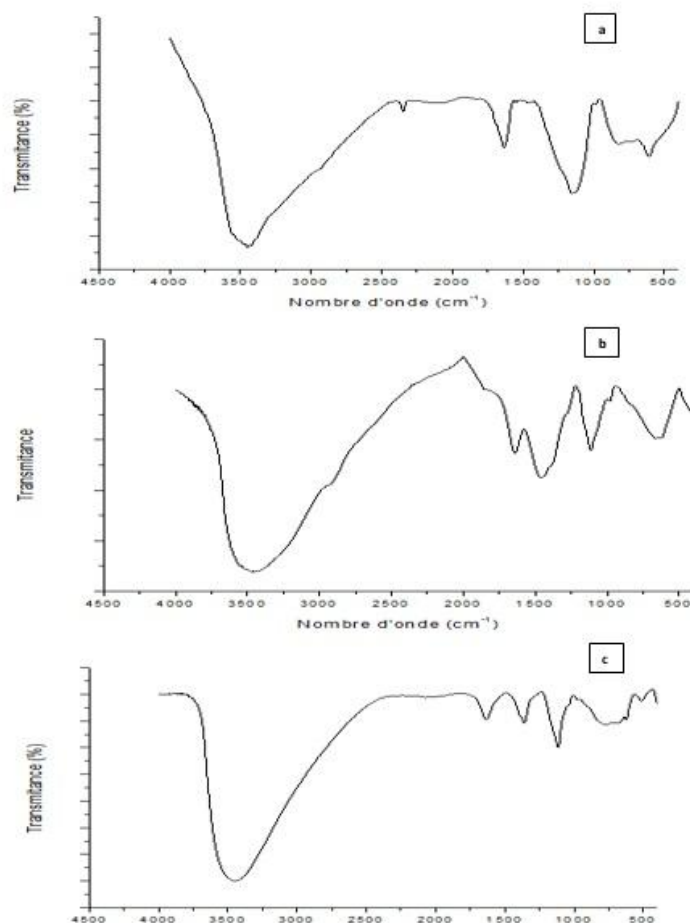


**Figure 8.** IR spectrum of sludge produced from EC with: a) Al/Al electrodes , b) precipitate deposited on Al cathode, c) Fe/ Fe electrodes

### 3.4.3 Scanning electron microscopy analysis :

A physical morphology study was performed on the sludge formed during the EC with Al/Al electrodes and Fe/Fe electrodes (figure 9) by SEM. The images analyzed at low magnification 5  $\mu\text{m}$  (figures. 9.a and 9.b) illustrate a rough, dense and wrinkled surface. At a magnification of 10  $\mu\text{m}$  (figure. 9.c), we clearly notice an irregular shape of the particles of sludge with a fuzzy crystalline edge. This irregularity is due to the very low degree of crystallinity of the compound which has an amorphous morphology. This aspect has also been observed by several authors [41], [43], [44]. This confirms the conclusions of X-ray and infrared diffraction spectrum analyzes, relating to the amorphous character of the sludge formed during the EC at the Al/Al electrodes.

The images of sludge produced with Fe/Fe electrodes in figure 9 show that the grains or nanocrystals of the nickel-iron hydroxide carbonate are characterized by an agglomeration of small particles as well as a different morphology and size. It is possible to observe the formation of lamellar crystals or aggregated platelet particles with superposition of layers. The lower resolution of the generated images is probably due to the low conductivity of the formed compound.

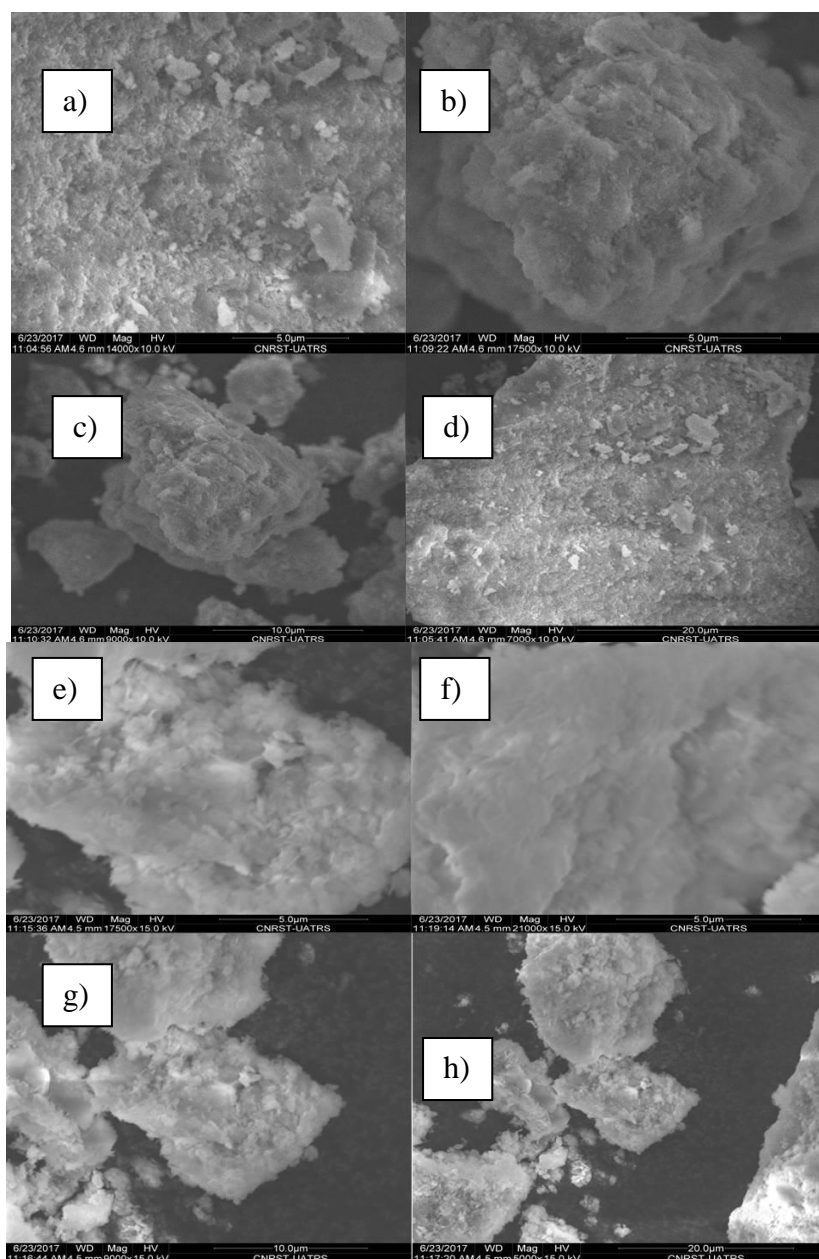


**Figure 9.** SEM images characterizing the sludge formed by EC with Al/Al electrodes(a,b : 5 $\mu$ m), (c : 10 $\mu$ m) and (d : 20  $\mu$ m) and Fe/Fe electrodes (e,f : 5 $\mu$ m), (g : 10 $\mu$ m) and (h : 20  $\mu$ m)

#### 4. Conclusion

This study shed light on the applicability of the EC technique in the treatment of wastewater from an electroplating unit. We studied the influence of variables, such as the voltage, the nature of the electrode material, the stirring speed and the interelectrode distance on nickel removal. Experimental results revealed that the elimination of  $\text{Ni}^{2+}$  metal ions by EC is better with aluminum electrodes (removal rate of 78%) than with iron electrodes (68% removal rate) under an optimum voltage of 6 volts. The results obtained under varying operating conditions showed that the efficiency of the removal was significantly affected by the applied voltage. Under high tension, the amount of formed metal hydroxide flocs increases and act as adsorbents where the  $\text{Ni}^{2+}$  metal ions are attached. The precipitate  $\text{Ni}(\text{OH})_2$  formed on the aluminum electrodes confirms that the elimination of  $\text{Ni}^{2+}$  ions is done by precipitation in the form of amorphous nickel hydroxide (hydroxyl ions formed at the cathode during the electrolysis of the water) and by co-

precipitation with aluminum hydroxides. X-ray diffraction, infrared spectroscopy, and SEM images helped us to identify the sludge resulting from EC. Indeed, the compound formed during the EC with Al/Al electrodes is nickel hydroxide with an amorphous morphology. In addition, the compound formed during the EC with the Fe/Fe electrodes is  $\text{Fe}_2\text{Ni}_2(\text{CO}_3)(\text{OH}) \cdot 8.2\text{H}_2\text{O}$  (Nickel Iron Carbonate Hydroxide Hydrate) which is a corrosion inhibitor.

## References

- [1] M. A. Barakat, *Arab. J. Chem.*, 4 (4) (2011) 361–377.
- [2] T. A. Kurniawan, G. Y. S. Chan, W. H. Lo, S. Babel, *Chem. Eng. J.*, 118 (1–2) (2006) 83–98.
- [3] A. E. Lewis, *Hydrometallurgy*, 104 (2) (2010) 222–234.
- [4] B. Mavis, 'Homogeneous precipitation of nickel hydroxide powders', Iowa state University, 2003.
- [5] D. Zamboulis, E. N. Peleka, N. K. Lazaridis, K. A. Matis, *J. Chem. Technol. Biotechnol.*, 86 (3) (2011) 335–344.
- [6] F. Zidane, B. Berrada, B. Lekhlif, M. Lounès, J. Blais, *J. Environ. Eng. Sci.*, 327 (4) (2006) 317–327.
- [7] I. Kabdaşlı, I. Arslan-Alaton, O. Tünay, *Environ. Technol.*, 1 (1) (2012) 2–45.
- [8] M. M. Emamjomeh, M. Sivakumar, *J. Hazard. Mater.*, 131(1) (2006) 118–125.
- [9] G. Chen, *Sep. Purif. Technol.*, 38 (1) (2004) 11–41.
- [10] M. Zaied, N. Bellakhal, *J. Hazard. Mater.*, 163 (1) (2009) 995–1000.
- [11] F. Ozyonar, *Int. J. Electrochem. Sci.*, 11 (1) (2016) 1456–1471.
- [12] A. A-mohammed, *Iraq. J. Chem. Pet. Eng.*, 9 (3) (2008) 37–41.
- [13] M. Bayramoglu, M. Eyvaz, M. Kobya, *Chem. Eng. J.*, 128 (1) (2007) 155–161.
- [14] K. Rajeshwar, *J. Appl. Electrochem.*, 24 (12) (1994) 1077–1091.
- [15] M. Y. A. Mollah, P. Morkovsky, J. A. G. Gomes, M. Kesmez, J. Parga, D. L. Cocke, *J. Hazard. Mater.*, 114 (1) (2004) 199–210.
- [16] A. E. Yilmaz, R. Boncukcuo, M. M. Kocakerim, *J. Hazard. Mater.*, 125(1) (2005) 160–165.
- [17] A. D. M. Ferreira, M. Marchesiello, P. Thivel, *Sep. Purif. Technol.*, 107 (1) (2013) 109–117.
- [18] N. Daneshvar, A. Oladegaragoze, N. Djafarzadeh, *J. Hazard. Mater.*, 129 (1) (2006) 116–122.
- [19] F. Zidane, P. Drogui, B. Lekhlif, J. Bensaid, J. F. Blais, S. Belcadi, K. El kacemi, *J. Hazard. Mater.*, 155 (1–2) (2008) 153–163.
- [20] F. Akbal, S. Camciotless, *Desalination*, 269 (1–3) (2011) 214–222.
- [21] N. Beyazit, *Int. J. Electrochem. Sci.*, 9 (1) (2014) 4315–4330.
- [22] L. Oudrhiri, F. Zidane, J. F. Blais, *J. Mater. Environ. Sci.*, 5(1) (2014) 111–120.
- [23] I. Heidmann and W. Calmano, *Sep. Purif. Technol.*, 71(3) (2010) 308–314.
- [24] N. Meunier, P. Drogui, C. Gourvenec, G. Mercier, R. Hausler, J-F. Blais, *Environ. Technol.*, 3330 (1) (2017) 235–245.
- [25] D. Ghernaout, A. I. Al-ghonamy, M. Wahib, *J. Electrochem. Sci. Eng.*, 4(4) (2014) 271–283.
- [26] B. Lekhlif, L. Oudrhiri, F. Zidane, P. Drogui, and J. F. Blais, *J. Mater. Environ. Sci.*, vol. 5, no. 1, pp. 111–120, 2014.
- [27] K. Dermentzis, E. Valsamidou, A. Lazaridou, N. C. Kokkinos, *J. Eng. Sci. Technol. Rev.*, 4 (2) (2011) 188–192.
- [28] N. Danesh, H. Ashassi-sorkhabi, A. Tizpar, *Sep. Purif. Technol.*, 31(1) (2003) 153–162.
- [29] O. Larue, E. Vorobiev, C. Vu, B. Durand, *Sep. Purif. Technol.*, 31(2) (2003) 177–192.
- [30] W. D. Callister, J. Wiley, Materials Science, 7 th ed., New york, 2007.
- [31] M. Ilou, F. Abida, Z. Hatim, A. Kheribech, *Med. J. Chem.*, 5(4) (2016) 521–527.

- [32] K. Missaoui, W. Bouguerra, C. Hannachi, B. Hamrouni, *J. Wat. Res. Protec.*, 5(1) (2013) 867–875.
- [33] L. Zaleschi, C. Teodosiu, I. Cretescu, M. A. Rodrigo, *Environ. Eng. Manag. J.*, 11(8) (2012) 1517–1525.
- [34] O. T. Can, M. Bayramoglu, M. Kobya, *Ind. Eng. Chem. Res.*, 2 (4) (2003) 3391–3396.
- [35] S. Vasudevan, J. Lakshmi, G. Sozhan, *Des.*, 310 (1) (2013) 122–129.
- [36] K. Brahmi, W. Bouguerra, M. Loungou, Z. Tlili, *Arab. J. Chem.*, (2015).
- [37] J. Duan, J. Gregory, *Adv. Colloid. Interfac. sc.*, 102(1) (2003) 475–502.
- [38] A. Prasetyaningrum, B. Jos, Y. Dharmawan, B. T. Prabowo, *J. Phys.*, 6 (1) (2018).
- [39] E. Uzunova, D. Klissurski, S. Kassabov, *J. Mater. Chem.*, 4 (1) (1994) 153–159.
- [40] J. L. Bantignies S. Deabate, A. Righi, S. Rols, P. Hermet, J. L. Sauvajol, F. Henn, *J. Phys. Chem. C.*, 112(6) (2008) 2193–2201.
- [41] H. B. Li, M.H. Yu, F.X. Wang, P. Liu, Y. Liang, J. Xiao, C. X. Wang, Y. X. Tong, G. W. Yang, *Nat. Commun.*, 4(1894) (2013) 1–7.
- [42] P. Hermet, L. Gourrier, J.-L. Bantignies, D. Ravot, T. Michel, S. Deabate, P. Boulet, F. Henn, *Phys. Rev.*, 84(23) (2011) 1–10.
- [43] C. Liu, S. Chen, Y. Li, *J. Rare Earths*, 28(2) (2010) 265–269.
- [44] C. Liu, P. Li, S. Chen, Y. Li, *Integr. Ferroelectr.*, 135(1) (2012) 30–38.